Extraterrestrial chromite in the resurge deposits of the early Late Ordovician Lockne crater, central Sweden

Alwmark, Carl; Schmitz, Birger

Published in:
Earth and Planetary Science Letters

DOI:
10.1016/j.epsl.2006.10.034

2007

Available online at www.sciencedirect.com
ScienceDirect
Earth and Planetary Science Letters 253 (2007) 291 – 303
EPSL
www.elsevier.com/locate/epsl

Extraterrestrial chromite in the resurge deposits of the early Late Ordovician Lockne crater, central Sweden

Carl Alwmark *, Birger Schmitz

Department of Geology, University of Lund, Sölvegatan 12, SE-22362 Lund, Sweden

Received 1 June 2006; received in revised form 24 October 2006; accepted 24 October 2006
Available online 1 December 2006
Editor: R.W. Carlson

Abstract

The distribution of extraterrestrial chromite grains (>63 μm) has been studied in the resurge deposit of the early Late Ordovician (458 Ma) Lockne impact structure in central Sweden. A 1-kg-sample of resurge sediment from the rim of the crater is extremely rich in extraterrestrial chromite. In total the sample contains >125 chromium spinel grains kg^{-1}, most grains being chromite. Due to post-depositional alterations, the origin of several of the grains is dubious, although it is clear that the major part of the chromites is of extraterrestrial origin (>75 grains kg^{-1}), most likely derived from the impactor. The alterations are primarily due to the hydrothermal system induced by the impactor, with zinc enrichment in the chromites as the most common characteristic. The element chemistry of the least altered chromite grains indicates that the impactor was an ordinary L chondrite. This concurs with a suggested increase in the flux of L chondritic asteroids to Earth, following the disruption of the L chondrite parent body at ca. 470 Ma.

More than 170 impact craters are known from around the Earth, but only few of the impactors have been identified, mainly due to the low survival rate of projectile material. Further studies of impact craters will reveal if survival of extraterrestrial chromite is unique for the Lockne structure.

Keywords: L chondrite; extraterrestrial chromite; impact crater; Late Ordovician; ordinary chondritic asteroid

1. Introduction

More than 170 impact craters are known on Earth [1] (a current listing is available on the internet, see the "Earth Impact Database" at: (http://www.unb.ca/passc/ImpactDatabase/), but only a fraction of the impactors have been identified. This is mainly due to the low survival rate of projectile material [2]. Physical pieces of projectile material have, with a few exceptions such as the Eltanin impact event [3], only been found at small (<1.5 km in diameter) impact craters [4–6]. Larger projectiles are believed to be totally vaporized upon impact, leaving only a small amount of recondensed projectile vapour mixed in with the target rocks (e.g., [7]). Factors that can affect the survival extent are the impact velocity [8], angle of impact [9], the type of impactor and impact target material. Pieces of meteorites have a low resistance towards weathering and diagenesis; most meteorites do not survive more than between a few thousand years to a couple of hundred of thousand years on the Earth surface [7,10].

* Corresponding author. Tel.: +46 46 2227877; fax: +46 46 2224419.
E-mail address: carl.alwmark@geol.lu.se (C. Alwmark).

0012-821X/$ - see front matter © 2006 Elsevier B.V. All rights reserved.
doi:10.1016/j.epsl.2006.10.034

Attempts to identify the type of impactor have previously focused on the geochemistry of the impact rocks hosting the recondensed fraction. Studies include measurements and interelement ratios of siderophile elements, primarily the platinum group elements (PGE) (e.g., [11–15]) and Cr-isotope measurements (e.g., [16–18]). Both these methods have limitations and are not always successful in the identification of impactor type. The siderophile trace element analysis becomes less useful if the host rocks have an original high enrichment in PGEs, masking the extraterrestrial component, e.g. as in the case of the Botsumtwi crater [19]. The comparison of interelement ratios is also complicated by the sometimes heterogeneous element distribution in the impactites caused by fractionation processes during vaporization/condensation and post impact alteration/mobilization of the siderophile elements coupled to, for example, impact-induced hydrothermal systems [6,20,21]. For the detection of extraterrestrial Cr isotopes, a large part of the chromium in the impactites has to be of extraterrestrial origin to show an effect that is larger than the precision of the measurement. The method is also complicated, and because of the very small differences in isotopic composition, the precision of the measurements has to be extremely high [18].

In this study a sample of the resurge deposit that forms part of the 458 Ma Lockne impact structure in central Sweden (Fig. 1) has been examined in search of physical material from the impactor. The resurge deposit is strongly enriched in Ir (up to 4.5 ppb) [22], suggesting presence of up to 0.9 wt.% (calculated on the assumption that the impactor had about 500 ppb Ir) of extraterrestrial matter either in a recondensed or relict state. The search has focused on chromite ($FeCr_2O_4$), a common accessory mineral in many meteorites [23]. Chromite has a high resistance against weathering and diagenesis and is often the only mineral surviving in chondritic fossil meteorites [24,25]. Chromite is also a

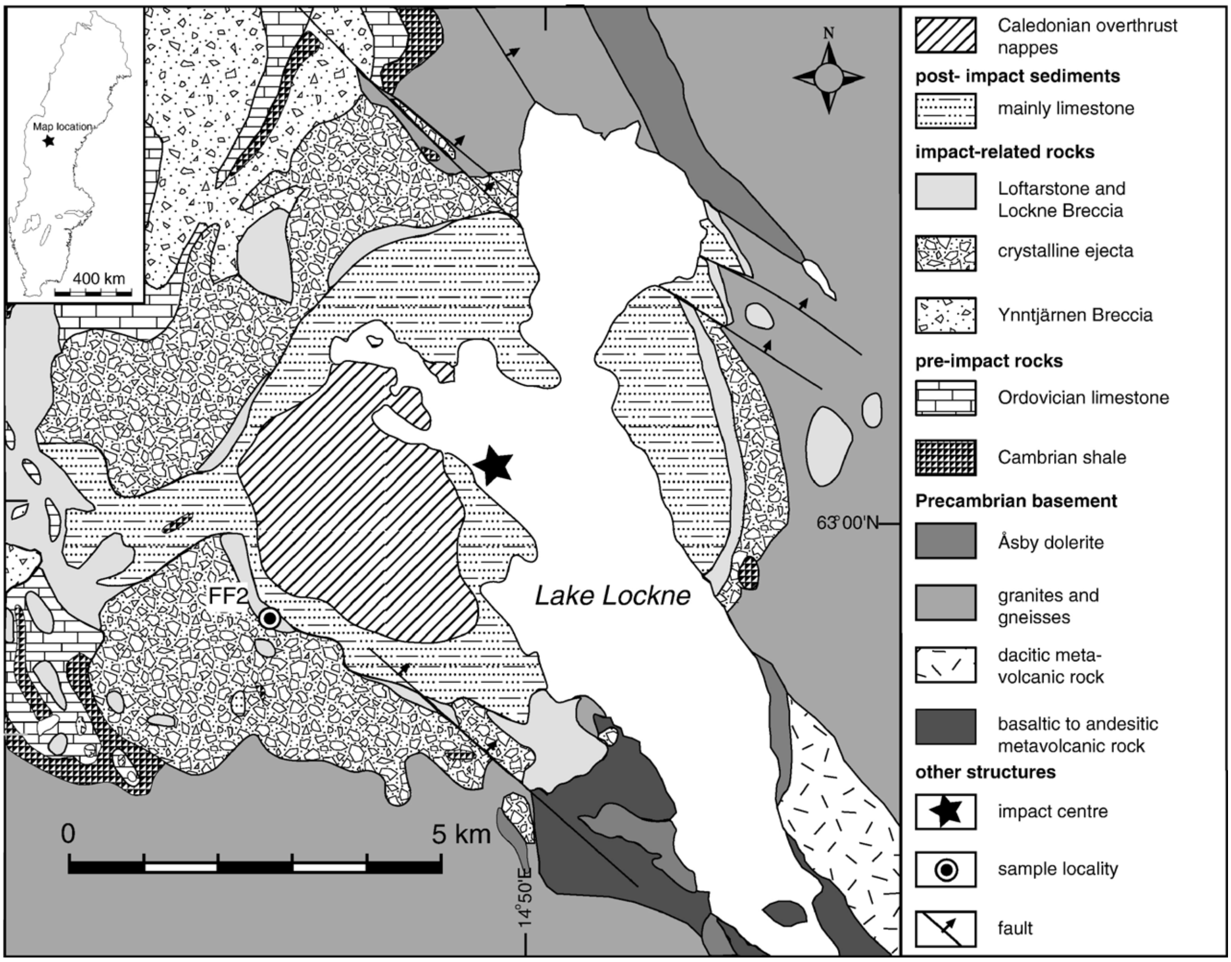

Fig. 1. Geological map of the Lockne area in central Sweden, simplified after Lindström et al. [37].

good petrogenetic indicator; extraterrestrial (chondritic) chromite (EC) has a characteristic composition that differs from the terrestrial chromite, with typically higher TiO_2 content (2.0–3.5 wt.%) and Cr/(Cr+Al) ratio (>0.8) and a narrow span of V_2O_3 (0.6–0.9 wt.%) (for further details see [26,27]). Furthermore, the compositions within the EC vary slightly with type of host meteorite [28]. Presence of EC in the Lockne resurge deposits could therefore be helpful in the identification of the type of impactor.

2. Geological setting

2.1. The Lockne impact structure

The Lockne impact structure in the Jämtland province, central Sweden (N 63°00′, E 14°49′; Fig. 1) is a well preserved concentric crater formed in the early Late Ordovician, at about 458 Ma [29]. The age is revised compared to earlier literature based on the 2004 Geological Time Scale [30]. The impacting body has been calculated to have been about 600 m in diameter, striking the sea surface at an oblique angle at intermediate water depth (500–1000 m) [31–34]. The composition of the target seafloor was that of sedimentary rocks (~80 m thick), mainly shale and limestone [35], overlying the crystalline basement. The impact structure consists of an inner crater, 7.5 km in diameter, surrounded by an 1–2.5 km wide and up to 50 m thick brim [36,37]. The brim consists exclusively of ejected, more or less brecciated, crystalline local basement, mostly granitoids from the Revsund Suite together with lesser parts of volcanites, gneisses and dolerites [37,38]. The brim is cut by at least four resurge gullies, formed when the water rushed back into the newly formed crater [39]. In parts of the outer breaches of the brim the crystalline ejecta is overlying a mostly monomictic limestone breccia, the Ynntjärnen Breccia. The breccia was generated by a water crater expanding outside of the inner crater [37].

The impact also generated an instant, rather short lived, hydrothermal circulation system of low temperature, with large volumes of fluids flowing through the breccia and the shattered basement [40]. The system promoted in situ crystallization of calcite, quartz, chalcopyrite, pyrite and sphalerite in the cavities and fractures [40], all which are present in the studied sample.

2.2. The Lockne resurge deposits

Because the Lockne impact took place in the sea, parts of the ejecta blanket were reworked and incorporated in resurge deposits, thus this being a good place to look for traces of the impacting body, especially considering the high Ir content of the deposits.

The resurge deposits are subdivided into two main lithologies: the Lockne Breccia and the Loftarstone [37]. The Lockne Breccia is a clast-supported breccia, with clasts ranging in size from sub-millimetres to hundreds of cubic meters. It is dominated by limestone, but clasts of crystalline basement and shales are also present. It is poorly sorted and bedding is absent [37]. The Lockne Breccia is more than 155 m thick in the centre of the crater, thinning outwards [39]. The Loftarstone, directly overlying the Lockne Breccia, constitutes a ca. 45 m thick sequence in the centre of the crater, representing the final phase of the resurge [39]. It is a greywacke-like arenitic rock with a grain size ranging from coarse sand to silt in a fining upward sequence [41]. The Loftarstone has roughly the same composition as the Lockne Breccia, although it has a larger proportion of crystalline material [36,41]. It also contains material interpreted as impact generated melt and abundant shocked quartz [42]. Iridium analyses of five samples of the Loftarstone show a distinct anomaly, with concentrations from 0.8 ppb to 4.5 ppb [22]. The Ir correlates well with Cr, implying that the two elements have a common origin, i.e. the impactor (Fig. 2) [22].

3. Materials and methods

In this study 950 g of the Loftarstone with a known high concentration of Ir (2.5 ppb) and Cr (72 ppm) was chosen, sample FF2 (Fig. 3a–b) [22]. Sample FF2 originates from a resurge deposit at the edge of the inner crater (N 62°59′90″, E 14°45′34″), 3.5 km from the centre (Fig. 1) [22]. The sample was decalcified in 6 M hydrochloric acid at room temperature. The residue was

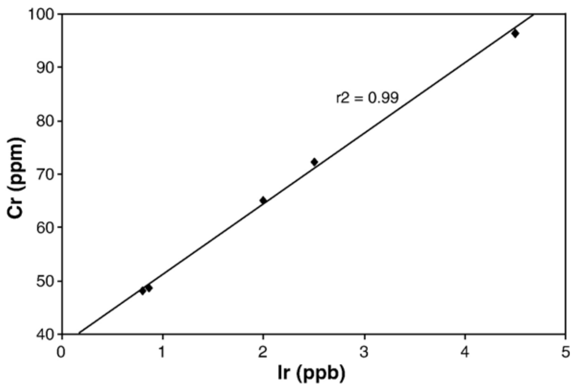

Fig. 2. The correlation between Cr and Ir in five different samples of the Loftarstone. Data from Sturkell [22].

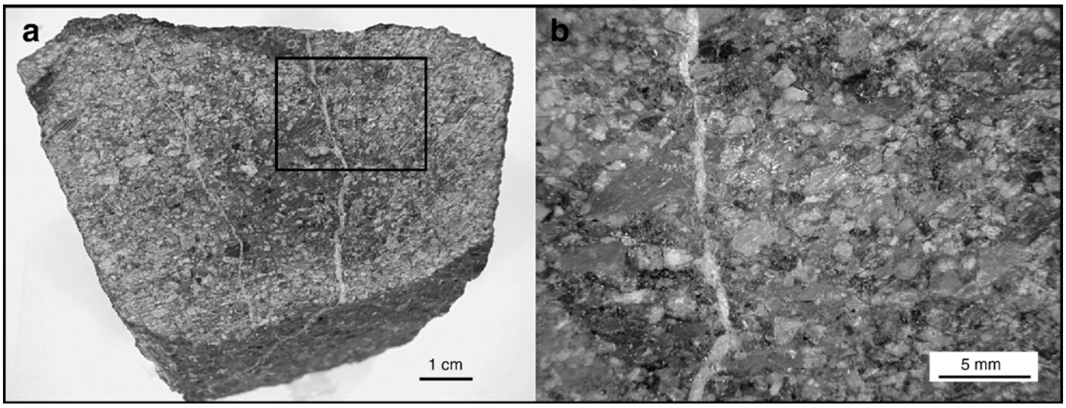

Fig. 3. a) The Loftarstone (sample FF2); b) close-up view of the texture. The fracture is filled with calcite.

then sieved at 63 μm and the recovered fraction leached in 18 M hydrofluoric acid at room temperature. The residual >63 μm fraction was dried and then heated in an oven at 550 °C for 24 h. The heating destroys coal particles that can be misidentified as chromite grains. Extensive tests have shown that the heating does not affect the chemical composition of the chromite grains. The residue after the heating was studied under an optical microscope and suspected chromite grains were picked for elemental analyses. The grains were mounted in epoxy resin and polished flat using a 1 μm diamond slurry. Four thin sections of FF2 were also made in order to search for "in situ" chromite and, if possible, to find other relict cosmic material.

Quantitative elemental analyses were performed with an energy dispersive spectrometer detector (EDS) linked to a scanning microscope with a Ge detector, each grain was analysed three times at different locations. Cobalt was used for standard; the acceleration voltage was 16 kV and the current 2.5 nA. X-ray mapping was carried out on grains suspected to be heterogeneous or not in equilibrium. The precision of the analyses was between 1 and 4%, and the accuracy was controlled by regular analyses of the USNM 117075 chromite reference standard [43]. The concentration of ferric iron was calculated using the formula (XY_2O_4) and based on the assumption of perfect stoichiometry, where X=Fe^{2+}, Ni, Mn, Mg, Zn and Cu and Y=Cr, Al, V and Fe^{3+}; Ti is calculated as being in an ulvöspinel component. Thus the values of ferric iron should be treated with caution.

Geological maps of the surroundings of the Lockne area were studied in search for possible contaminating terrestrial chromite sources, mainly mafic and ultra mafic rocks. Thin sections were made of four suspected chromite bearing rocks; a heavily altered brecciated dolerite dyke (N 62°55′59″, E 14°47′49″), an Åsby dolerite (N 62°55′27″, E 15°09′05″), a fine-grained amphibolite (N 62°50′22″, E 15°00′15″) and a porphyroblastic amphibolite (N 62°52′26″, E 14°39′59″). The thin sections were systematically searched in a reflective light microscope and alleged chromites where analysed in an electron scanning microscope.

4. Results

A total of 119 chromium-rich spinels were found in the 950 g sample of the Loftarstone, giving a number of 125 grains kg^{-1}, this being a minimum amount, due to a minor loss of material because of incomplete sample dissolution. The grains are divided into five groups based on differences in chemical composition, listed in Table 1 and A1 (Fig. 4). These groups are extraterrestrial chromites (EC, 73 grains), other chromium-rich spinels (OC, 8 grains), oxidized chromite (OxC, 10 grains), oxidized chromite with high zinc (ZnC, 26 grains) and high aluminium chrome spinels (AlC, 2grains). In the thin sections of FF2, one chromium-rich grain was found "in situ"; it falls into the OxC group. Only one of the sampled mafic rocks in the surrounding area was chromite bearing, this being the brecciated and heavily altered dolerite dyke located ~8 km south of the impact centre. The compositions of these chromites are closest to that of the OxC group (Table 1 and A1).

4.1. Chemical composition and properties of the spinels

The EC grains have a mean size of about 100 μm in diameter and vary in shape from almost perfectly euhedral to anhedral (Fig. 5a). They are normally coarse but a few of the anhedral grains have an aggregate structure, consisting of smaller (5–10 μm) euhedral chromites. Irregular fractures and voids are common in

Table 1
The average element concentration (wt.% and standard deviation (1σ)) and the highest (max) and lowest (min) concentrations in the different groups of chromites and chromium-rich spinels from sample FF2 of the Loftarstone and the brecciated dolerite dyke

	TiO_2	V_2O_3	Al_2O_3	Cr_2O_3	FeO total	FeO	Fe_2O_3	MnO	MgO	Cu_2O	NiO	ZnO	Total	Cr/3+ [a]
Loftarstone EC (73 grains)														
Mean	2.48±0.38	0.72±0.05	5.74±0.75	57.87±1.09	26.83±1.84	26.83±1.84	0.00	1.44±0.47	1.59±1.54	0.00	0.05±0.14	2.35±2.10	99.07±1.01	87.12±1.47
Max	3.08	0.80	6.56	61.15	31.15	30.98	0.17	2.56	5.81	0.00	0.62	7.28	101.38	92.93
Min	1.56	0.58	2.87	55.88	22.28	22.28	0.00	0.64	0.00	0.00	0.00	0.00	96.22	85.73
Loftarstone OC (8 grains)														
Mean	0.94±0.29	0.58±0.14	6.20±0.45	61.53±0.92	22.74±1.45	22.67±1.43	0.07±0.18	0.65±0.07	6.04±1.15	0.00	0.30±0.22	0.18±0.15	99.14±0.70	86.87±0.96
Max	1.28	0.76	7.08	62.93	24.60	24.60	0.51	0.75	7.78	0.00	0.78	0.35	99.98	88.31
Min	0.57	0.37	5.49	60.13	20.96	20.96	0.00	0.54	4.67	0.00	0.00	0.00	97.98	85.27
Loftarstone OxC (10 grains)														
Mean	1.01±0.36	0.90±0.34	5.79±0.86	47.76±3.78	36.56±4.09	27.64±3.16	8.92±3.73	2.19±0.52	0.19±0.35	0.00	0.00	3.99±2.08	98.38±0.89	73.6±6.09
Max	1.59	1.33	6.96	52.07	46.24	31.01	15.24	3.13	1.00	0.00	0.00	9.38	99.53	80.8
Min	0.21	0.23	4.01	41.04	32.95	19.41	5.18	1.29	0.00	0.00	0.00	1.74	96.33	63.6
Loftarstone ZnC (26 grains)														
Mean	0.9±0.30	0.76±0.17	5.92±0.62	45.67±1.86	18.83±3.05	9.29±2.01	9.54±1.18	1.16±0.19	0.00	0.91±0.26	0.00	24.27±2.01	98.43±1.46	71.82±2.00
Max	1.55	1.03	8.15	49.09	25.34	13.23	12.11	1.52	0.00	1.67	0.00	28.45	99.91	75.40
Min	0.43	0.26	5.12	41.96	12.77	5.35	7.42	0.86	0.00	0.49	0.00	20.70	94.03	67.61
Loftarstone AlC (2 grains)														
1	0.51	0.00	16.55	42.03	36.35	31.17	5.18	1.29	1.13	0.00	0.24	0.00	98.10	58.67
2	0.16	0.00	13.89	50.68	26.09	22.44	3.65	2.08	6.03	0.00	0.18	0.00	99.11	67.70
Brecciated dolerite dyke (2 grains)														
1	0.89	0.18	5.08	38.66	50.29	29.44	20.85	1.47	0.35	0.00	0.00	1.73	98.65	58.5
2	0.92	0.18	4.30	38.25	51.12	29.72	21.40	1.44	0.25	0.00	0.00	1.15	97.61	58.8

[a] Cr/3+: mol% Cr/(Cr+Al+Fe^{3+}).

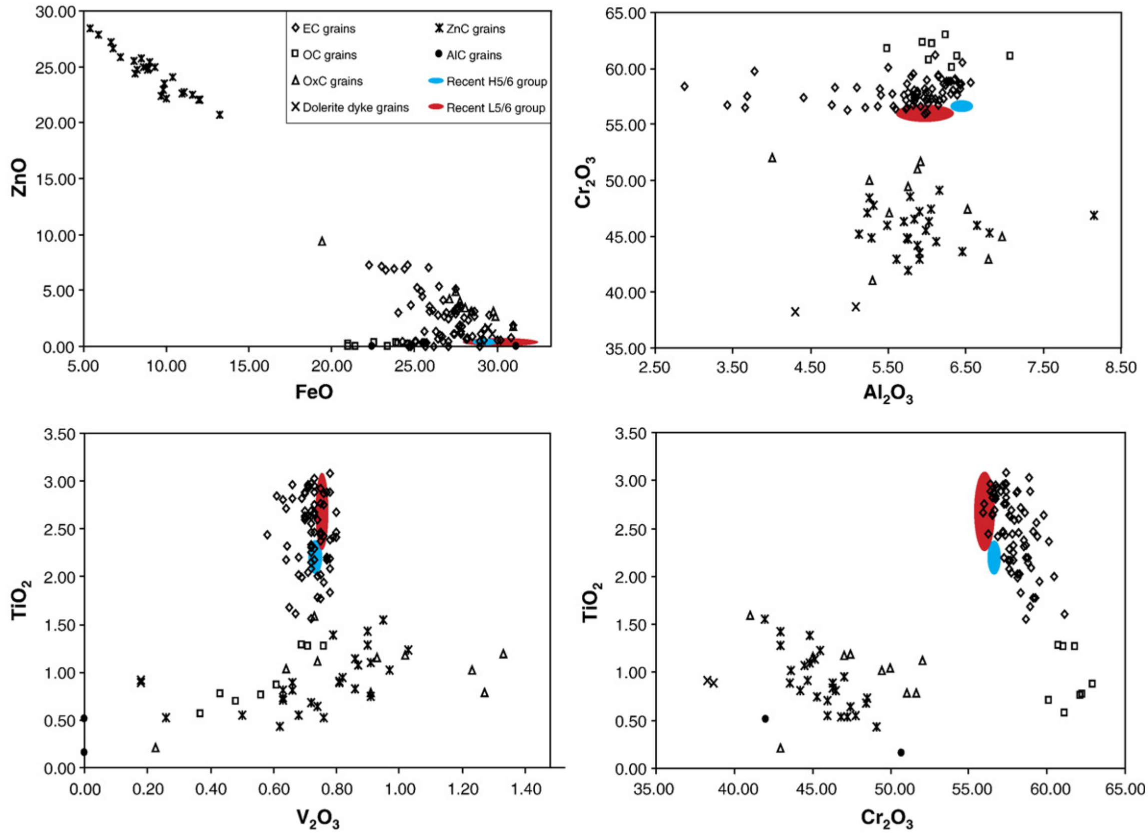

Fig. 4. Chemical composition of individual Cr-spinels in wt.%. Shown is also the average composition, with standard deviation fields, of chromite grains from 12 recent L5/6 meteorites and 13 recent H5/6 meteorites, data from Schmitz et al. [27].

the grains, the voids are rounded, irregular and do not show any conformity with the lattice of the host crystal. Inclusions are rare, although some of the voids might have hosted inclusions that were destroyed by the hydrofluoric acid. Of the few inclusions present, quartz and feldspar dominate. The grains generally show little variation in chemistry, with high Cr_2O_3 (56–61 wt.%), low Al_2O_3 (3–7 wt.%) and MgO (0–6 wt.%), relatively high TiO_2 (1.5–3 wt.%) and a narrow span of V_2O_3 (0.6–0.8 wt.%). FeO varies between 22 and 31 wt.% with a mean of 27 wt.% and MnO between 0.6 and 2.6 wt.%. ZnO fluctuates between 0 and 7 wt.%, where the grains with high zinc tend to have a more porous surface (see below).

The OC grains are anhedral, with a mean diameter of 100 μm (Fig. 5b). They are analogous in appearance and composition to the aggregate EC grains, with the exception of lower amounts of TiO_2 (0.6–1.3 wt.%), FeO (mean 23 wt.%) and MnO (0.5–0.8 wt.%), slightly higher Cr_2O_3 (60–63 wt.%) and MgO (5–8 wt.%) plus minor amounts of NiO. Concentrations of ZnO are very low or absent (0–0.4 wt.%).

The OxC grains have a mean diameter of about 90 μm, are euhedral to subhedral and coarse (Fig. 5c). The composition is characterized by the presence of iron in trivalent state (Fe_2O_3 5–15 wt.%), which is negatively correlated to Cr_2O_3 (41–51 wt.%). MgO is very low or absent (0–1 wt.%) while ZnO (2–9 wt.%) is always present. TiO_2 concentrations are relatively lower than in the EC (0.2–1.6 wt.%). The ZnC grains are generally more homogenous in appearance than the OxC grains, but similarly euhedral to subhedral and coarse (Fig. 5d). The composition also resembles that of the OxC, but with unusually high ZnO values between 20–28 wt.% together with small amounts of CuO (0.5–1.7 wt.%) and a total lack of MgO.

Fractures, voids and inclusions are common in both the OxC and the ZnC grains. Two types of voids are present; irregular voids, as in the EC grains, and angular voids. The angular voids have a negative crystal structure. The inclusions are generally very small (<5 μm), preventing quantitative elemental analysis without influence of the host mineral. Nonetheless, inclusions of quartz, feldspar, rutile and Fe–Ti-oxides, have been

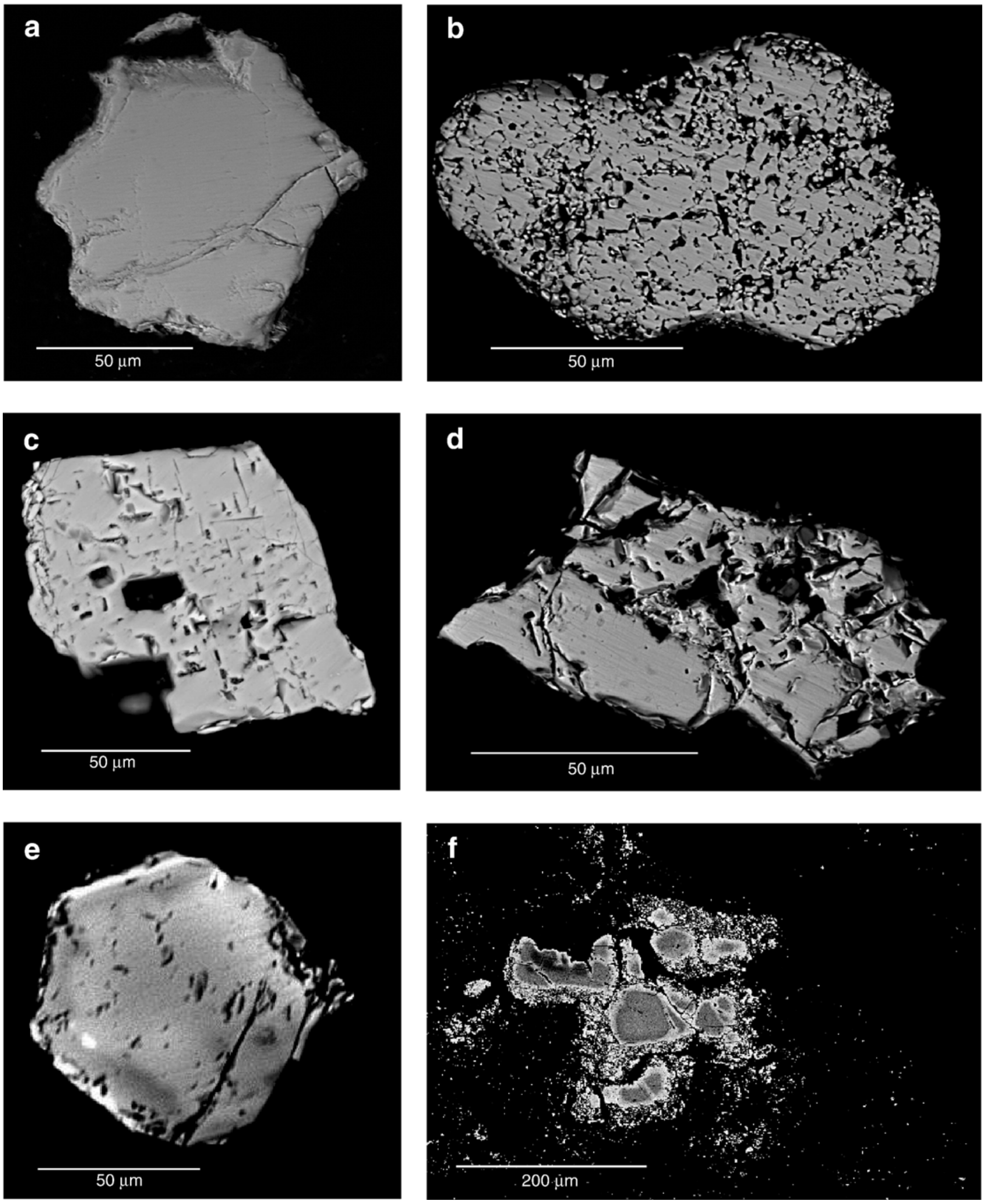

Fig. 5. Backscatter images of the different Cr-spinels. a–e are from the Loftarstone, f is from the brecciated dolerite dyke. a) Subhedral coarse EC grain; b) OC with aggregate structure; c) OxC with angular voids and inclusions of rutile along the crystal structure of the host mineral; d) ZnC with both angular and rounded voids; e) euhedral AlC; f) Cr-spinel from the brecciated dolerite dyke, with an outer rim of ferritchromite and an outermost partial rim of magnetite.

determined. The quartz and feldspar inclusions are in the form of rounded grains or as a partial filling in the irregular voids. The rutile and Fe–Ti-oxides are angular and usually conforming to the lattice of the host crystal. The rutile is also present as exsolution-like lamellae, oriented along the crystallographic planes of the spinel. Probably some of the voids, both the rounded and angular, once hosted inclusions that have either weathered away or been dissolved by the hydrofluoric acid.

The two AlC grains are ~80 μm in diameter, non-porous, coarse and euhedral (Fig. 5e). They have a homogenous composition with relatively high Al_2O_3, 14 and 17 wt.%, in contrast to the almost constant values around 6 wt.% of the EC grains in the sample. The AlC grains contain no ZnO or V_2O_3 and the TiO_2 values are low (0.2 and 0.5 wt.%).

The spinel from the nearby brecciated dolerite has a core with a composition close to that of the OxC in FF2, but with a lower Cr/Fe^{3+}. The core is surrounded by an inner rim of ferritchromite with decreasing Cr/Fe^{3+} and minor amounts of zinc, and an outer incomplete rim of almost pure magnetite (Fig. 5f).

Some of the studied grains are chemically heterogeneous and sometimes show zoning. For example, some EC grains show a zoning from core to rim (Fig. 6). The zoning pattern is characterized by an enrichment of Zn in the rim of the grain. The boundary between the rim and the core is almost always sharp and the zoning is

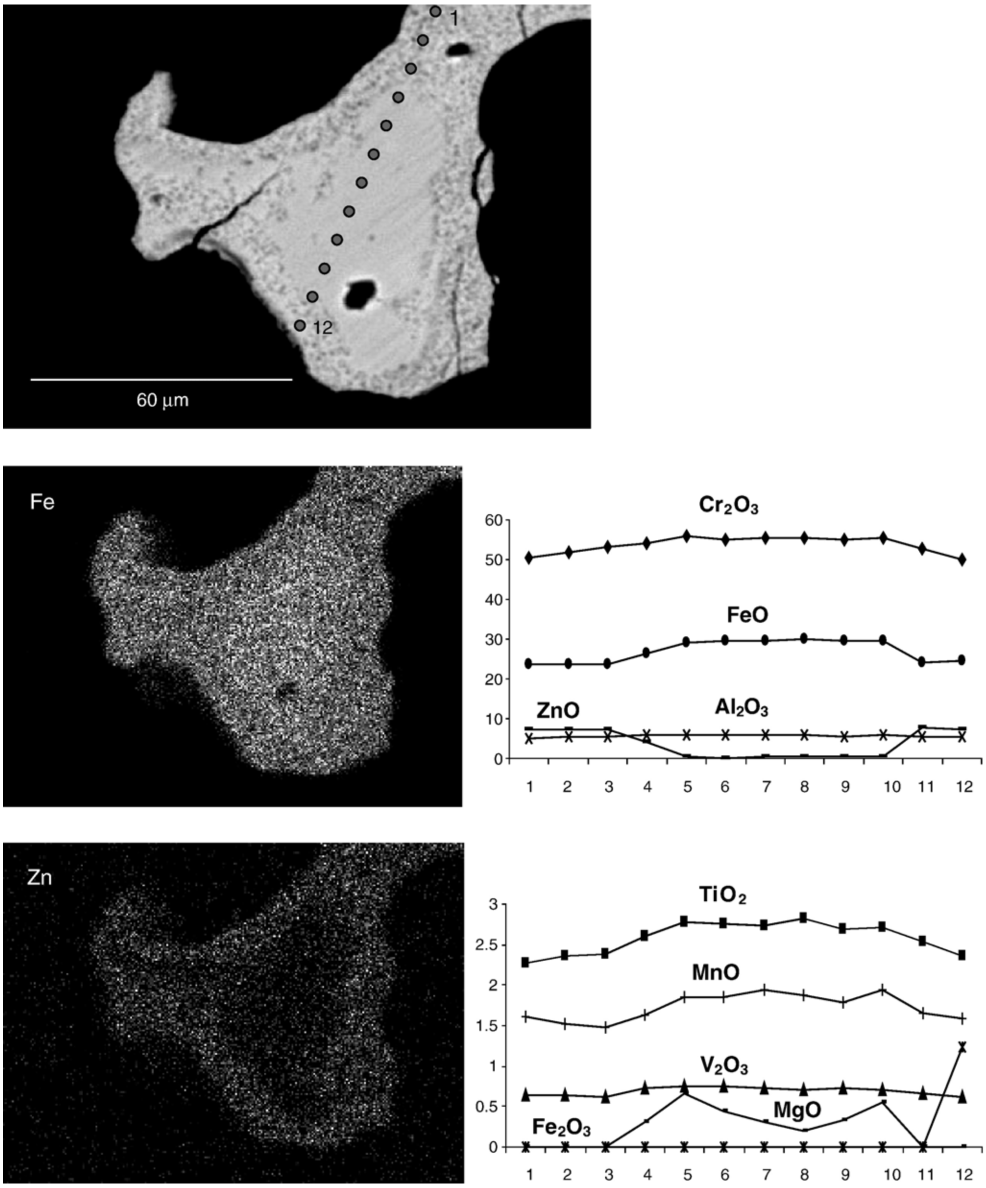

Fig. 6. Transect and X-ray mapping of a diagenetically altered EC grain from the Loftarstone with an enrichment of zinc in the rim. Note the porous appearance of the altered rim.

distinguished optically by the rim being porous compared to the more solid core. The higher Zn values are proportional to particularly lower Mg and Fe^{2+} and to some extent Ti, V and Cr, whereas Al does not seem to be affected. Some of the OxC grains exhibit a zoning pattern, with a narrow rim, enriched in Fe^{3+}, Fe^{2+} and Ti and depleted in Cr and to some extent Al, Zn and Mg (Fig. 7).

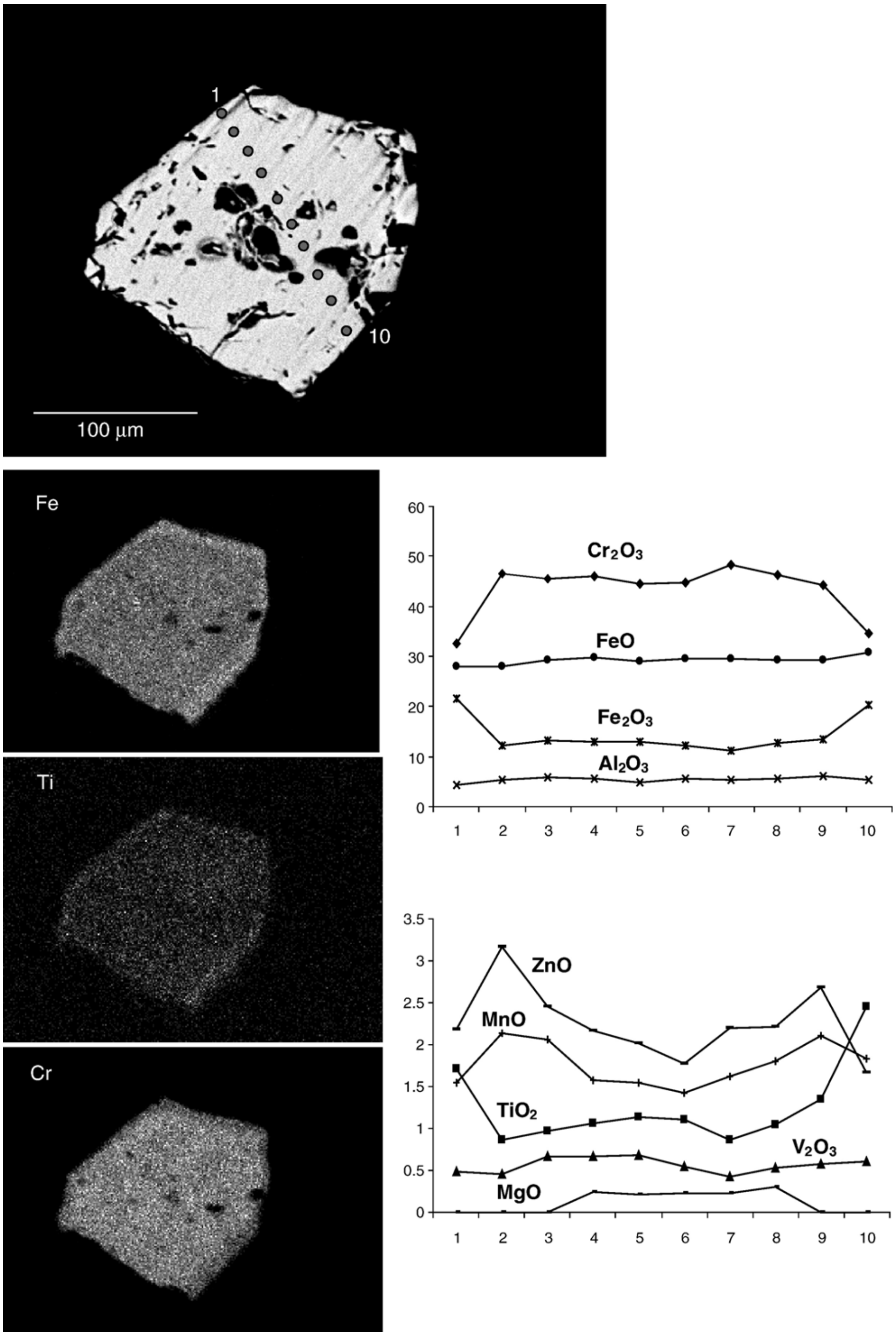

Fig. 7. Transect and X-ray mapping of an OxC grain from the Loftarstone with an enrichment of titanium and ferric iron in the rim.

5. Discussion

5.1. Origin and alteration of the spinels

The presence of chemical zoning, pitted surfaces and exsolutions, imply that several of the spinels in this study have been subdued to alterations. Modification of spinel is not uncommon and chromite, although being comparably very resistant to diagenesis, can be affected by hydrous alterations and metamorphism [44]. This is especially true for spinels with high Fe and Cr content, as in this case, since they have an inverse spinel structure that is less stable and more sensitive to alteration [45].

Although several of the spinel grains in this study are affected by diagenetic alteration, the majority of the grains (73 of 119) have a well-preserved, typical EC (i.e. chondritic) composition. The average composition of the 73 grains classified as EC is almost identical to the average composition of 594 chromite grains from 26 fossil Ordovician meteorites from Kinnekulle in southern Sweden (Table 2) [27]. The concentration of EC grains in the Lockne sample is too high to represent reworked EC grains from ordinary mid-Ordovician marine limestone. Mid-Ordovician limestone may contain enhanced concentrations of EC related to the increased background influx of smaller meteorites following the disruption of the L chondrite parent body at 470 Ma [46,47]. However, the richest limestone beds examined by Schmitz et al. [47] in the quarries at Kinnekulle have ca. 3 sediment-dispersed EC grains kg^{-1}; hence the majority of the EC grains in this study most likely derive from the body that created the Lockne impact structure. If one assumes that the average chromite grain is a cube with a length of 100 μm, a density of 4.6 g cm^{-3} and that an ordinary chondrite has an average chromite content of 0.27 wt.% [48], the amount of EC grains would correspond to about 0.13 g of meteoritic material kg^{-1} in the Loftarstone sample studied. The quantity of resurge deposit has been estimated to 13 km^3 [49] and the density about 2.6 g cm^{-3} [50], this would give ca. 4.4 million metric tonnes of meteoritic material embedded in the resurge deposit, assuming an average of 75 chromite grains kg^{-1} throughout the deposit. This corresponds to 1.15% of the impactor (calculated on a 600 m diameter impact body with an average ordinary chondrite density of 3.4 g cm^{-3} [51]). The same calculations based on the Ir measurements, assuming 2.5 ppb Ir throughout the resurge deposit and an impactor with 500 ppb Ir gives ca. 170 million metric tonnes of meteoritic material in the resurge deposits, corresponding to 44% of the impactor. The low percentage of meteoritic material calculated on EC, compared to the results of the Ir, is probably due to a loss

Table 2
The average element concentration (wt.% and standard deviation) of the Loftarstone EC grains in comparison with other studies

	Cr_2O_3	Al_2O_3	MgO	TiO_2	V_2O_3	FeO	MnO	ZnO	Fe#[a]	Cr#[b]
EC grains from sample FF2 of the Loftarstone, 73 grains, this study	57.87±1.09	5.74±0.75	1.59±1.54	2.48±0.38	0.72±0.05	26.83±1.84	1.44±0.47	2.35±2.10	90.4±8.1	87.1±1.5
Sediment-dispersed EC grains from Thorsberg quarry, Kinnekulle, 276 grains, Schmitz and Häggström [25]	57.61±1.58	6.07±0.76	2.58±0.79	3.09±0.33	0.75±0.07	27.36±2.63	0.78±0.2	0.53±0.5	85.6±3.90	86.5±1.42
EC grains from 26 meteorites from Thorsberg quarry, Kinnekulle, 594 grains, Schmitz et al. [27]	57.60±1.30	5.53±0.29	2.57±0.83	2.73±0.40	0.73±0.03	26.94±3.89	1.01±0.33	1.86±2.43	85.3±5.02	87.5±0.60
Chromite from 12 recent H5/6 group chondrites, Schmitz et al. [27]	56.64±0.37	6.44±0.14	2.98±0.23	2.20±0.17	0.73±0.02	29.27±0.67	1.00±0.08	0.33±0.05	84.7±1.2	85.5±0.3
Chromite from 12 recent L5/6 group chondrites, Schmitz et al. [27]	56.00±0.65	5.97±0.43	2.93±0.97	2.68±0.40	0.75±0.02	30.22±2.23	0.83±0.10	0.30±0.07	85.3±4.92	86.3±0.77
Chromite from 13 recent H4-6 group chondrites, Wlotzka [56]	57.1±1.10	6.64±0.41	3.4±0.18	1.96±0.29	0.65±0.03	28.9±0.60	0.88±0.07	0.28±0.14	82.7±1.00	85.2±1.00
Chromite from 6 recent L4-6 group chondrites, Wlotzka [56]	56.1±0.80	5.9±0.19	2.52±0.21	2.67±0.44	0.7±0.06	30.9±0.60	0.63±0.08	0.34±0.06	87.3±1.00	86.5±0.30
Chromite from 4 recent LL3-7 group chondrites, Wlotzka [56]	55.8±0.56	5.52±0.17	1.85±0.14	3.4±0.57	0.67±0.10	31.6±0.62	0.51±0.04	–	90.5±0.90	87.2±0.20

[a] Fe#: mol% Fe/(Fe+Mg).
[b] Cr#: mol% Cr/(Cr+Al).

of chromite through vaporization, melting and alteration during the impact and in the following hydrothermal system, as well as the fact that only grains larger than 63 μm were recovered in this study.

A detailed comparison of the chemical composition of the EC grains found in the Loftarstone with analyses of chromite from recent and fossil chondrites implies that the impactor was an ordinary chondrite of the L group (Table 2). The main argument for an L chondritic origin is the high TiO_2 content of 2.5 wt.% of the EC grains, which is close to the average TiO_2 content of 2.7 wt.% in chromite of recent L4-6 chondrites and fossil L chondrites from Kinnekulle, but relatively higher than the on average 2.0–2.2 wt.% TiO_2 of recent H4-6 chondrites (Table 2). The lower TiO_2 content and concomitantly slightly higher Cr/(Cr+Al) values (Table 2) compared to recent L chondrites probably reflects post depositional alterations. A weak negative correlation trend between Cr_2O_3 and TiO_2 (Fig. 4) is also seen in the most strongly weathered chromites from fossil meteorites at Kinnekulle [27]. Thus removing the 10 grains with the highest $Cr_2O_3/(Cr_2O_3+TiO_2)$, i.e. the presumably most altered grains, gives a mean of 2.6 wt.% for TiO_2. The lower averages of FeO and MgO on behalf of ZnO and MnO in the Loftarstone EC (Table 2) reflect that these elements typically are most affected by post depositional alterations, seen also in the data for Kinnekulle fossil meteorites [27]. On the whole the EC from the Loftarstone shows greater similarities to chromite from mid-Ordovician fossil meteorites than coeval sediment-dispersed EC grains. For example, the incorporation of Zn and Mn has, as a whole, been more extensive in the fossil meteorites and the Loftarstone chromites compared to sediment-dispersed chromite grains (Table 2). This most likely reflects that both the Loftarstone and fossil meteorite chromites weathered in anoxic to suboxic conditions, involving sulfide precipitation, whereas the sediment-dispersed lay on the oxidized sea floor before being buried [25].

The Lockne impactor being an L chondrite concurs with the suggestion that the influx of L chondritic asteroids to Earth was increased by up to one order of magnitude during the mid-Ordovician following the disruption of the L chondrite parent body at ca. 470 Ma [27,46]. As many as four of the seventeen impact craters known on the Baltoscandian shield formed during the Middle to early Late Ordovician, and the Lockne crater is one of them (the others are Kärdla, Tvären and Granby). The meteorite and micrometeorite flux during the same period may have been enhanced by up to two orders of magnitude [27,47].

The origin of the OC grains is somewhat unclear, although Cr/(Cr+Al) as high as 87 imply that they can be of extraterrestrial origin. The grains tend to follow the trend seen in the EC with higher Cr_2O_3 on behalf of TiO_2 (Fig. 4), which implies that the OC grains may originate from the impactor. Furthermore, clusters of chromite aggregates is a type only present in ordinary chondrites [52], thus the fact that most of the OC grains have an aggregate structure, supports an origin from the impactor. The unequilibrated state of some of the OxC reveals that the grains had an initially higher Cr and Mg content (Fig. 7). The depletion of Cr can also be seen in the "in situ" grain, found in a Loftarstone thin section, where the matrix surrounding the grain contains low amounts of Cr, not present further away from the specific grain. Whether the OxC had an initial Cr content and composition corresponding to that of chromite from the impactor or a terrestrial source is not possible to determine, thus neither the origin of the grains. The ZnC have been much altered; exsolutions, the absence of pores and the homogeneity of most of the grains imply that they are more or less recrystallized, thus it is not possible to determine their origin. The two AlC grains contain no Zn and seem to be rather unaffected by alterations. It is not possible to rule out the AlC grains as being extraterrestrial since ordinary chondrites contain also chromian spinels of very varying character. These are, however, rare making up for only 1–2% of the total Cr-rich oxides in chondrites [24].

The major modifications of the spinels, Zn enrichment and oxidation, are most likely a result of the hydrothermal system that was induced by the impact. The Caledonian overthrusting, although not very influential in the Lockne area, with only very low grade metamorphism [53], may have further altered the spinels. The degree of alteration of a specific spinel grain in the hydrothermal system is mainly related to the extent to which the grain has been exposed to fluids, which is dependent on the presence of cavities, cracks and fissures. As in the case of Zn, an element that is almost always secondary in Cr-spinels and often associated with metasomatic alterations coupled to sulphide mineralization [54], the ZnC grains with very high and homogeneous Zn concentrations have probably been the least sheltered.

5.2. Survival of extraterrestrial material

It is clear that the general assumption that physical fragments of the impactor are not to be expected at craters larger than ~1.5 km [4–6], does not apply for the Lockne impact structure. The fact that the impact was oblique, probably somewhere between 30 and 60° [34] have most likely increased the survival rate of material. That the target was overlain by water can also be a factor affecting the survival positively, as in the case of the Eltanin impact, where physical pieces of the impactor were retrieved [55]. However, one must keep in mind that the water depth at Lockne was only on the order of a tenth of that of the Eltanin impact (~5000 m); furthermore the Eltanin impact did not form a crater on the ocean floor [55]. Another factor that could have increased the survival rate, although not known, is if the impact was of low velocity due to atmospheric break up. Studies of other craters have been initiated in order to determine whether the survival of chromite at the Lockne impact is a unique phenomenon, due to these special circumstances.

6. Conclusions

The Loftarstone, part of the resurge deposits in the early Late Ordovician (458 Ma) Lockne impact structure, in central Sweden, is locally extremely rich in extraterrestrial chromite grains (>75 grains kg^{-1}), deriving from the impactor. Spinel grains in the Loftarstone have been subdued to post-depositional alterations primarily due to the hydrothermal system that was induced by the impact. The dominating alteration effect is the incorporation of Zn in the grains mainly on behalf of Mg and Fe^{2+}. The chemical composition of the best preserved grains indicates that the impactor was an ordinary chondrite of the L group. This concurs well with the hypothesis that the influx of asteroids to Earth was increased during the late Middle and early Late Ordovician because of the major disruption of the L chondrite parent body at ca. 470 Ma.

Further studies of terrestrial impact craters with resurge deposits will reveal if survival of chromite is unique for the Lockne impact structure.

Acknowledgements

We thank E. Sturkell and K. Högdahl for providing samples. We thank P. Claeys for helpful comments. This study was supported by grants from the Swedish Research Council and National Geographic Society.

Appendix A. Supplementary data

Supplementary data associated with this article can be found, in the online version, at doi:10.1016/j.epsl.2006.10.034.

References

[1] R.A.F. Grieve, The terrestrial cratering record, in: B. Peucker-Ehrenbrink, B. Schmitz (Eds.), Accretion of Extraterrestrial Matter Throughout Earth's History, Kluwer Academics, New York, 2001, pp. 379–402.

[2] R.A.F. Grieve, L.J. Pesonen, Terrestrial impact craters: their spatial and temporal distribution and impacting bodies, Earth Moon, Planets 72 (1996) 357–376.

[3] F.T. Kyte, D.E. Brownlee, Unmelted meteoritic debris in the Late Pliocene Ir anomaly: evidence for the impact of a nonchondritic asteroid, Geochim. Cosmochim. Acta 49 (1985) 1095–1108.

[4] H.J. Melosh, Atmospheric breakup of terrestrial impactors, in: P.H. Schultz, P.B. Merrill (Eds.), Multi-Ring Basins, Pergamon, New York, 1981, pp. 29–35.

[5] R.A.F. Grieve, Extraterrestrial impact events: the record in the rocks and the stratigraphic column, Palaeogeogr. Palaeoclimatol. Palaeoecol. 132 (1997) 5–23.

[6] C. Koeberl, Identification of meteoritic component in impactites, in: M.M. Grady, R. Hutchinson, G.H.J. McCall, R.A. Rothery (Eds.), Meteorites: Flux with Time and Impact Effects, Geol. Soc. Lond. Spec. Pub., vol. 140, 1998, pp. 133–153.

[7] M-J. Muñoz-Espadas, J. Martínez-Frías, R. Lunar, Main geochemical signatures related to meteoritic impacts in terrestrial rocks: a review, in: C. Koeberl, F. Martínez-Ruiz (Eds.), Impact Markers in the Stratigraphic Record, Springer-Verlag, Berlin, 2003, pp. 65–90.

[8] H.J. Melosh, Impact Cratering; A Geologic Process, Oxford Monographs on Geology and Geophysics, vol. 11, Oxford University Press, 1989, 245 pp.

[9] E. Pierazzo, H.J. Melosh, Hydrocode modelling of oblique impacts: the fate of the projectile, Meteorit. Planet. Sci. 35 (2000) 117–130.

[10] P.A. Bland, Terrestrial weathering rates defined by extraterrestrial materials, J. Geochem. Explor. 88 (2006) 257–261.

[11] J.W. Morgan, M.J. Janssens, J. Hertogen, J. Gros, H. Takahashi, Ries impact crater, southern Germany — search for meteoritic material, Geochim. Cosmochim. Acta 43 (1979) 803–815.

[12] H. Palme, M.J. Janssens, H. Takahashi, E. Anders, J. Hertogen, Meteoritic material at five large impact craters, Geochim. Cosmochim. Acta 42 (1978) 313–323.

[13] H. Palme, R.A.F. Grieve, R. Wolf, Identification of the projectile at the Brent crater and further considerations of projectile types at terrestrial craters, Geochim. Cosmochim. Acta 45 (1981) 2417–2424.

[14] G. Schmidt, H. Palme, K.L. Kratz, Highly siderophile elements (Re, Os, Ir, Ru, Rh, Pd, Au) in impact melts from three European impact craters (Sääksjärvi, Mien and Dellen) clues to the nature of the impacting bodies, Geochim. Cosmochim. Acta 61 (1997) 2977–2987.

[15] R. Tagle, P. Claeys, An ordinary chondrite impactor for the Popigai crater, Siberia, Geochim. Cosmochim. Acta 69 (2005) 2877–2889.

[16] A. Shukolyukov, G.W. Lugmair, Isotopic evidence for the Cretaceous–Tertiary impactor and its type, Science 282 (1998) 927–929.

[17] A. Shukolyukov, G.W. Lugmair, C. Koeberl, W.U. Reimold, Chromium in the Morokweng impact melt: isotopic evidence for extraterrestrial components and type of impactor, Meteorit. Planet. Sci. 34 (1999) A-107–A-108.

[18] C. Koeberl, B. Peucker-Ehrenbrink, W.U. Reimold, A. Shukolyukov, G.W. Lugmair, Comparison of Os and Cr isotopic methods for the detection of meteoritic components in impactites: examples from the Morokweng and Vredefort impact structures, South Africa, in: C. Koeberl, K.G. MacLeod (Eds.), Catastrophic Events and Mass Extinctions: Impacts and Beyond, Geol. Soc. Am. Spec. Pap., vol. 356, 2002, pp. 607–617.

[19] W.B. Jones, Chemical analyses of Bosumtwi crater target rocks compared with the Ivory Coast tektites, Geochim. Cosmochim. Acta 49 (1985) 2569–2576.
[20] M.W. Wallace, V.A. Gostin, R.R. Keays, Acraman impact ejecta and host shales; evidence for low-temperature mobilization of iridium and other platinoids, Geology 18 (1990) 132–135.
[21] N.J. Evans, D.C. Gregoire, R.A.F. Grieve, W.D. Goodfellow, J. Veizer, Use of platinum group elements for impactor identification: terrestrial impact craters and Cretaceous–Tertiary boundary, Geochim. Cosmochim. Acta 57 (1993) 3737–3748.
[22] E.F.F. Sturkell, Impact related Ir anomaly in the Middle Ordovician Lockne impact structure, Jämtland, Sweden, GFF 120 (1998) 333–336.
[23] A.E. Rubin, Mineralogy of meteorite groups, Meteorit. Planet. Sci. 32 (1997) 231–247.
[24] P. Thorslund, F.E. Wickman, J.O. Nyström, The Ordovician chondrite from Brunflo, central Sweden. I. General description and primary minerals, Lithos 17 (1984) 87–100.
[25] B. Schmitz, T. Häggström, Extraterrestrial chromite in Middle Ordovician marine limestone at Kinnekulle, southern Sweden — traces of a major asteroid breakup event, Meteorit. Planet. Sci. 41 (2006) 455–466.
[26] J.O. Nyström, M. Lindström, F.E. Wickman, Discovery of a second Ordovician meteorite using chromite as a tracer, Nature 336 (1988) 572–574.
[27] B. Schmitz, M. Tassinari, B. Peucker-Ehrenbrink, A rain of ordinary chondritic meteorites in the early Ordovician, Earth Planet. Sci. Lett. 194 (2001) 1–15.
[28] T.E. Bunch, K. Keil, K.G. Snetsinger, Chromite composition in relation to chemistry and texture of ordinary chondrites, Geochim. Cosmochim. Acta 31 (1967) 1569–1582.
[29] Y. Grahn, J. Nõlvak, F. Paris, Precise chitinozoan dating of Ordovician impact events in Baltoscandia, J. Micropaleontol. 15 (1996) 21–35.
[30] R.A. Cooper, P.M. Sadler, The Ordovician period, in: F.M. Gradstein, J.G. Ogg, A.G. Smith (Eds.), A Geological Time Scale 2004, Cambridge University Press, 2004, pp. 165–187.
[31] J. Ormö, M. Lindström, When a cosmic impact strikes the seabed, Geol. Mag. 137 (2000) 67–80.
[32] J. Ormö, H. Miyamoto, Computer modelling of the water resurge at a marine impact: the Lockne crater, Sweden, Deep-Sea Research II 49 (2002) 983–994.
[33] V. Shuvalov, J. Ormö, M. Lindström, Hydrocode simulation of the Lockne marine target impact event, in: C. Koeberl, H. Henkel (Eds.), Impact Tectonics, Springer-Verlag, Berlin, 2005, pp. 405–422.
[34] M. Lindström, V. Shuvalov, B. Ivanov, Lockne crater as a result of marine-target oblique impact, Planet. Space Sci. 53 (2005) 803–815.
[35] E.F.F. Sturkell, The marine Lockne impact structure, Jämtland, Sweden: a review, Geol. Rundsch. 87 (1998) 253–267.
[36] E.F.F. Sturkell, Resurge morphology of the marine Lockne impact crater, Jämtland, central Sweden, Geol. Mag. 135 (1998) 121–127.
[37] M. Lindström, J. Ormö, E.F.F. Sturkell, I. von Dalwigk, The Lockne crater: revision and reassessment of structure and impact stratigraphy, in: C. Koeberl, H. Henkel (Eds.), Impact Tectonics, Springer-Verlag, Berlin, 2005, pp. 357–388.
[38] M. Lindström, E.F.F. Sturkell, Geology of the Early Palaeozoic Lockne impact structure, Central Sweden, Tectonophysics 216 (1992) 169–185.
[39] M. Lindström, E.F.F. Sturkell, R. Törnberg, J. Ormö, The marine impact crater at Lockne, Central Sweden, GFF 118 (1996) 193–206.
[40] E.F.F. Sturkell, C. Broman, P. Forsberg, P. Torssander, Impact-related hydrothermal activity in the Lockne impact structure, Jämtland, Sweden, Eur. J. Mineral. 10 (1998) 589–606.
[41] S. Simon, Stratigraphie, Petrographie und Entstehungsbedingungen von Grobklastika in der autochthonen, ordovizishen Schichtenfolge Jämtlands (Schweden), Sver. Geol. Unders., Ser. C Avh. Uppsats. 815 (1987) 1–156.
[42] A. Therriault, M. Lindström, Planar deformation features in quartz grains from the resurge deposit of the Lockne structure, Sweden, Meteorit. Planet. Sci. 30 (1995) 700–703.
[43] E. Jarosewich, J.A. Nelen, J.A. Norberg, Reference samples for electron microprobe analysis, Geostand. Newsl. 4 (1980) 43–47.
[44] S.J. Barnes, Chromite in komatiites, II. Modification during greenschist to mid-amphibolite facies metamorphism, J. Petrol. 41 (2000) 387–409.
[45] D.J.M. Burkhard, Accessory chrome spinels: their co-existence and alteration in serpentinites, Geochim. Cosmochim. Acta 57 (1993) 1297–1306.
[46] E.V. Korochantseva, M. Trieloff, A.I. Buikin, C.A. Lorenz, M.A. Ivanova, W.H. Schwarz, J. Hopp, E.K. Jessberger, L chondrite asteroid breakup tied to Ordovician meteorite shower by multiple isochron ^{40}Ar–^{39}Ar dating, Meteorit. Planet. Sci. 41 (2006) A99.
[47] B. Schmitz, T. Häggström, M. Tassinari, Sediment-dispersed extraterrestrial chromite traces a major asteroid disruption event, Science 300 (2003) 961–964.
[48] K. Keil, On phase composition of meteorites, J. Geophys. Res. 67 (1962) 4055–4061.
[49] E.F.F. Sturkell, M. Lindström, Mass balance of the Lockne impact structure, central Sweden, GFF 118 (1996) A102–A103.
[50] R. Törnberg, E.F.F. Sturkell, Density and magnetic susceptibility of rocks from the Lockne and Tvären marine impact structures, Meteorit. Planet. Sci. 40 (2005) 639–651.
[51] S.L. Wilkison, M.S. Robinson, Bulk density of ordinary chondrite meteorites and implications for asteroidal internal structure, Meteorit. Planet. Sci. 35 (2000) 1203–1213.
[52] P. Ramdohr, The Opaque Minerals in Stony Meteorites, Elsevier, Amsterdam, 1973, 245 pp.
[53] I. Bryhni, P.G. Andréasson, Metamorphism in the Scandinavian Caledonides, in: D.G. Gee, B.A. Sturt (Eds.), The Caledonide Orogen — Scandinavia and Related Areas, J. Wiley & Sons Ltd., 1985, pp. 763–781.
[54] L.R. Bernier, Vanadiferous zincian–chromian hercynite in a metamorphosed basalt-hosted alteration zone, Atik Lake, Manitoba, Can. Mineral. 28 (1990) 37–50.
[55] R. Gersonde, F.T. Kyte, U. Bleil, B. Diekmann, J.A. Flores, G. Grahl, R. Hagen, G. Kuhn, F.J. Sierros, D. Volker, A. Abelmann, J. A. Bostwick, Geological record and reconstruction of the late Pliocene impact of the Eltanin asteroid, Nature 390 (1997) 357–363.
[56] F. Wlotzka, Cr spinel and chromite as petrogenetic indicators in ordinary chondrites: equilibration temperatures of petrologic types 3.7 to 6, Meteorit. Planet. Sci. 40 (2005) 1673–1702.

Appendix

Table A1
Element concentration (wt%) of the different chromites and chromium-rich spinels from sample FF2 of the Loftarstone and the brecciated dolerite dyke. The values are the mean of three different analysis points in each grain. In the heterogeneous grains the analyses where performed in parts that where assumed to have the most primary composition, most often in the central parts of the grain.

Loftarstone EC grains														
#	**TiO_2**	**V_2O_3**	**Al_2O_3**	**Cr_2O_3**	**FeO total**	**FeO**	**Fe_2O_3**	**MnO**	**MgO**	**Cu_2O**	**NiO**	**ZnO**	**Tot.**	**Cr#[1]**
1	2.64	0.71	5.83	57.57	22.99	22.99	0.00	1.70	0.00	0.00	0.00	7.13	98.57	86.9
2	2.87	0.70	5.57	56.57	23.28	23.28	0.00	1.77	0.00	0.00	0.00	6.78	97.54	87.2
3	2.75	0.76	6.06	57.23	27.77	27.77	0.00	1.95	0.60	0.00	0.00	1.92	99.04	86.4
4	2.46	0.75	5.73	57.18	27.79	27.79	0.00	1.23	1.48	0.00	0.00	1.08	97.70	87.0
5	1.78	0.74	6.14	59.25	25.47	25.47	0.00	0.77	4.97	0.00	0.48	0.34	99.94	86.6
6	2.38	0.78	6.43	58.53	25.60	25.60	0.00	0.90	3.51	0.00	0.00	1.34	99.47	85.9
7	2.56	0.72	5.80	59.32	24.80	24.80	0.00	1.49	0.90	0.00	0.00	3.72	99.31	87.3
8	2.88	0.73	5.83	57.07	26.92	26.92	0.00	1.37	1.40	0.00	0.00	3.00	99.20	86.8
9	2.62	0.70	5.70	57.64	27.47	27.47	0.00	1.19	1.13	0.00	0.00	2.87	99.32	87.2
10	2.44	0.75	6.03	57.80	27.35	27.35	0.00	1.02	2.80	0.00	0.00	1.07	99.26	86.5
11	2.20	0.68	5.74	58.67	26.43	26.43	0.00	0.70	3.35	0.00	0.00	0.62	98.39	87.3
12	2.60	0.70	5.39	58.21	25.18	25.18	0.00	1.99	0.51	0.00	0.00	5.22	99.80	87.9
13	1.94	0.76	5.82	59.53	25.73	25.73	0.00	0.66	3.48	0.00	0.35	0.39	98.66	87.3
14	2.82	0.69	5.84	57.37	26.44	26.44	0.00	1.48	1.69	0.00	0.00	2.75	99.08	86.8
15	1.99	0.69	6.43	58.13	28.21	28.21	0.00	1.07	3.42	0.00	0.00	0.81	100.75	85.8
16	2.44	0.58	4.97	56.26	23.75	23.75	0.00	1.62	0.62	0.00	0.00	6.96	97.20	88.4
17	2.17	0.77	6.20	57.88	25.92	25.92	0.00	1.33	1.45	0.00	0.00	3.14	98.86	86.2
18	2.09	0.72	6.00	59.01	24.67	24.67	0.00	0.71	4.76	0.00	0.62	0.00	98.58	86.8
19	1.77	0.75	6.36	59.10	24.60	24.60	0.00	0.76	4.76	0.00	0.58	0.27	98.95	86.2
20	3.03	0.73	6.25	58.85	26.81	26.81	0.00	2.29	0.25	0.00	0.00	2.64	100.85	86.3
21	1.61	0.67	6.10	61.15	25.68	25.68	0.00	0.84	5.33	0.00	0.00	0.00	101.38	87.1
22	2.69	0.70	5.36	56.62	29.55	29.55	0.00	0.98	0.60	0.00	0.00	2.77	99.27	87.6
23	1.56	0.72	6.42	58.67	26.75	26.75	0.00	1.22	2.89	0.00	0.31	0.46	99.00	86.0
24	2.02	0.75	6.33	58.09	27.45	27.45	0.00	1.09	2.56	0.00	0.00	1.11	99.40	86.0
25	3.08	0.78	5.96	57.37	25.89	25.89	0.00	1.97	0.00	0.00	0.00	3.61	98.66	86.6
26	2.89	0.77	6.06	58.12	27.07	27.07	0.00	1.97	0.00	0.00	0.00	2.48	99.36	86.5
27	2.19	0.78	6.56	58.76	27.71	27.71	0.00	2.09	0.25	0.00	0.00	1.75	100.09	85.7
28	2.69	0.72	5.88	57.74	25.41	25.41	0.00	1.68	0.33	0.00	0.00	4.98	99.43	86.8
29	2.04	0.71	6.31	57.69	26.75	26.75	0.00	1.51	0.85	0.00	0.00	4.11	99.97	86.0
30	2.41	0.79	6.14	59.38	26.54	26.54	0.00	1.10	1.76	0.00	0.20	1.02	99.34	86.6
31	1.68	0.65	6.35	58.92	26.70	26.70	0.00	1.08	2.54	0.00	0.00	0.93	98.85	86.2
32	2.08	0.78	6.39	57.58	27.63	27.63	0.00	2.04	0.00	0.00	0.00	3.23	99.73	85.8
33	2.95	0.71	5.98	57.19	29.27	29.27	0.00	1.08	1.14	0.00	0.00	1.54	99.86	86.5
34	2.33	0.72	5.99	57.88	27.24	27.24	0.00	1.40	0.75	0.00	0.00	2.91	99.22	86.6
35	2.59	0.74	5.88	57.94	22.28	22.28	0.00	1.61	0.00	0.00	0.00	7.28	98.32	86.9
36	2.75	0.73	5.86	57.35	27.51	27.51	0.00	2.56	0.28	0.00	0.00	3.32	100.36	86.8
37	2.89	0.78	6.28	58.89	28.53	28.53	0.00	1.81	0.22	0.00	0.00	0.86	100.26	86.3
38	2.47	0.72	6.19	59.12	26.28	26.28	0.00	1.05	2.12	0.00	0.00	1.29	99.24	86.5
39	2.67	0.80	6.21	58.57	27.03	27.03	0.00	1.81	0.37	0.00	0.00	0.45	97.91	86.4
40	2.82	0.66	3.66	56.50	25.86	25.86	0.00	1.77	0.19	0.00	0.00	7.04	98.50	91.2
41	2.17	0.64	3.68	57.52	27.72	27.72	0.00	1.25	0.53	0.00	0.00	3.41	96.92	91.3
42	2.81	0.63	3.43	56.72	24.41	24.41	0.00	1.88	0.00	0.00	0.00	6.96	96.84	91.7
43	2.37	0.75	5.50	60.13	24.00	24.00	0.00	1.36	2.24	0.00	0.00	3.05	99.40	88.0
44	2.87	0.76	5.84	58.03	29.01	29.01	0.00	1.42	1.50	0.00	0.00	1.15	100.58	87.0
45	2.64	0.72	3.78	59.77	27.90	27.90	0.00	1.53	1.28	0.00	0.00	1.81	99.43	91.4
46	2.65	0.73	5.20	56.51	27.49	27.49	0.00	1.67	0.62	0.00	0.00	5.13	100.00	87.9
47	2.72	0.64	2.87	58.34	31.15	30.98	0.17	1.75	0.57	0.00	0.00	1.91	99.95	92.9
48	2.29	0.73	5.40	57.57	25.45	25.45	0.00	1.68	0.45	0.00	0.00	4.46	98.03	87.7
49	2.97	0.72	5.60	56.35	28.24	28.24	0.00	1.62	1.04	0.00	0.00	2.34	98.88	87.1
50	2.00	0.74	6.45	60.47	24.80	24.80	0.00	0.67	2.70	0.00	0.42	0.00	98.25	86.3
51	2.02	0.68	4.82	58.25	26.51	26.51	0.00	1.74	0.37	0.00	0.00	5.36	99.75	89.0
52	2.96	0.66	4.41	57.40	28.61	28.61	0.00	1.93	0.53	0.00	0.00	2.73	99.23	89.7
53	2.88	0.77	5.78	57.41	28.15	28.15	0.00	1.99	0.67	0.00	0.00	0.72	98.37	87.0
54	2.47	0.73	6.16	57.18	27.84	27.84	0.00	1.80	1.22	0.00	0.00	1.33	98.73	86.2
55	2.15	0.72	6.31	58.82	25.08	25.08	0.00	0.65	2.27	0.00	0.35	0.40	96.73	86.2
56	2.84	0.61	4.77	56.71	24.61	24.61	0.00	1.81	0.00	0.00	0.00	7.26	98.61	88.9
57	2.33	0.65	6.44	58.67	25.64	25.64	0.00	0.75	1.17	0.00	0.31	0.29	96.22	85.9
58	2.64	0.70	5.74	56.50	26.08	26.08	0.00	1.64	1.86	0.00	0.00	3.21	98.37	86.8
59	2.67	0.73	5.97	55.88	27.73	27.73	0.00	1.66	0.84	0.00	0.00	3.60	99.08	86.3
60	2.92	0.71	5.92	56.57	30.22	30.22	0.00	1.69	1.34	0.00	0.00	0.57	99.94	86.5
61	2.96	0.71	6.11	57.29	28.19	28.19	0.00	1.24	2.14	0.00	0.00	0.65	99.29	86.3
62	2.31	0.72	6.24	58.51	24.26	24.26	0.00	0.78	5.81	0.00	0.00	0.45	99.08	86.3
63	2.25	0.72	5.75	57.85	25.11	25.00	0.11	0.81	5.65	0.00	0.22	0.43	98.79	87.0
64	2.43	0.76	6.01	57.31	28.93	28.93	0.00	1.79	1.59	0.00	0.00	0.48	99.30	86.5
65	2.88	0.70	5.73	56.40	28.45	28.45	0.00	1.97	0.00	0.00	0.00	3.14	99.27	86.8
66	2.92	0.75	6.14	56.77	30.06	30.06	0.00	1.78	0.76	0.00	0.00	0.57	99.75	86.1
67	2.46	0.80	5.97	58.20	28.93	28.93	0.00	0.99	2.28	0.00	0.00	0.00	99.63	86.7
68	2.41	0.80	6.01	56.85	28.03	28.03	0.00	1.47	1.62	0.00	0.00	2.55	99.74	86.4
69	2.95	0.73	5.82	56.72	30.86	30.86	0.00	2.15	0.00	0.00	0.00	0.79	100.02	86.7

70	2.76	0.75	6.00	56.01	28.67	28.67	0.00	1.96	0.37	0.00	0.00	3.09	99.61	86.2
71	2.17	0.73	5.56	57.67	27.08	27.08	0.00	0.99	4.32	0.00	0.00	0.00	98.52	87.4
72	2.20	0.77	6.21	57.25	29.21	29.21	0.00	1.09	3.10	0.00	0.00	0.56	100.39	86.1
73	1.83	0.78	5.10	58.29	26.18	26.18	0.00	0.64	3.72	0.00	0.00	0.00	96.54	88.5
Mean	2.48	0.72	5.74	57.87	26.83	26.83	0.00	1.44	1.59	0.00	0.05	2.35	99.07	87.1
Max.	3.08	0.80	6.56	61.15	31.15	30.98	0.17	2.56	5.81	0.00	0.62	7.28	101.38	92.9
Min.	1.56	0.58	2.87	55.88	22.28	22.28	0.00	0.64	0.00	0.00	0.00	0.00	96.22	85.7

Loftarstone OC grains

#	TiO_2	V_2O_3	Al_2O_3	Cr_2O_3	FeO total	FeO	Fe_2O_3	MnO	MgO	Cu_2O	NiO	ZnO	Tot.	Cr#
1	0.57	0.37	7.08	61.11	23.91	23.91	0.00	0.71	5.70	0.00	0.22	0.31	99.98	85.3
2	0.70	0.48	6.32	60.13	23.39	22.88	0.51	0.69	6.28	0.00	0.26	0.00	98.25	85.9
3	1.27	0.71	6.39	61.05	24.01	24.01	0.00	0.54	5.17	0.00	0.34	0.26	99.74	86.5
4	0.87	0.61	6.24	62.93	20.96	20.96	0.00	0.61	6.29	0.00	0.78	0.27	99.56	87.1
5	1.28	0.69	6.03	60.75	24.60	24.60	0.00	0.69	4.92	0.00	0.00	0.24	99.20	87.1
6	1.27	0.76	5.49	61.80	22.57	22.57	0.00	0.75	4.67	0.00	0.32	0.35	97.98	88.3
7	0.77	0.43	5.95	62.27	21.42	21.39	0.04	0.65	7.49	0.00	0.24	0.00	99.22	87.5
8	0.76	0.56	6.07	62.16	21.02	21.02	0.00	0.58	7.78	0.00	0.23	0.00	99.16	87.3
Mean	0.94	0.58	6.20	61.53	22.74	22.67	0.07	0.65	6.04	0.00	0.30	0.18	99.14	86.9
Max	1.28	0.76	7.08	62.93	24.60	24.60	0.51	0.75	7.78	0.00	0.78	0.35	99.98	88.3
Min	0.57	0.37	5.49	60.13	20.96	20.96	0.00	0.54	4.67	0.00	0.00	0.00	97.98	85.3

Loftarstone OxC grains

#	TiO_2	V_2O_3	Al_2O_3	Cr_2O_3	FeO total	FeO	Fe_2O_3	MnO	MgO	Cu_2O	NiO	ZnO	Tot.	Cr#
1	0.79	1.27	5.88	51.05	33.38	27.48	5.90	2.27	0.00	0.00	0.00	4.89	99.53	78.0
2	0.79	0.91	5.92	51.64	33.88	28.42	5.45	2.29	0.00	0.00	0.00	3.08	98.51	78.7
3	1.02	1.23	5.75	49.43	32.95	27.77	5.18	1.95	0.00	0.00	0.00	4.00	96.33	78.5
4	1.04	0.64	5.26	49.99	35.94	28.07	7.86	2.01	0.27	0.00	0.00	3.44	98.59	76.5
5	1.19	1.33	6.52	47.41	37.53	29.77	7.76	1.94	0.00	0.00	0.00	3.10	99.02	73.5
6	1.12	0.74	4.01	52.07	34.19	27.44	6.75	2.08	0.59	0.00	0.00	3.30	98.10	80.8
7	1.59	0.73	5.30	41.04	46.24	31.01	15.23	1.29	0.00	0.00	0.00	1.74	97.93	64.7
8	0.21	0.23	6.79	42.95	34.65	19.41	15.24	3.13	1.00	0.00	0.00	9.38	98.33	63.6
9	1.18	1.02	5.52	47.04	36.28	27.10	9.18	2.89	0.00	0.00	0.00	4.25	98.18	73.5
10	1.16	0.93	6.96	45.00	40.53	29.91	10.63	2.01	0.00	0.00	0.00	2.70	99.29	68.7
Mean	1.01	0.90	5.79	47.76	36.56	27.64	8.92	2.19	0.19	0.00	0.00	3.99	98.38	73.6
Max	1.59	1.33	6.96	52.07	46.24	31.01	15.24	3.13	1.00	0.00	0.00	9.38	99.53	80.8
Min	0.21	0.23	4.01	41.04	32.95	19.41	5.18	1.29	0.00	0.00	0.00	1.74	96.33	63.6
In situ grain	0.66	0.66	4.46	46.19	39.62	25.85	13.77	2.29	0.37	0.00	0.00	4.35	98.60	70.0

Loftarstone ZnC grains

#	TiO_2	V_2O_3	Al_2O_3	Cr_2O_3	FeO total	FeO	Fe_2O_3	MnO	MgO	Cu_2O	NiO	ZnO	Tot.	Cr#
1	1.55	0.95	5.75	41.96	25.34	13.23	12.11	1.25	0.00	0.69	0.00	20.70	98.19	67.6
2	0.89	0.66	5.90	43.53	18.77	9.69	9.08	1.09	0.00	0.78	0.00	22.41	94.03	71.4
3	0.68	0.72	5.26	48.44	15.12	6.75	8.37	1.08	0.00	1.32	0.00	26.59	99.21	75.4
4	1.10	0.91	5.74	44.83	21.24	10.36	10.88	1.28	0.00	0.49	0.00	24.05	99.64	70.3
5	1.14	0.86	5.12	45.15	22.12	10.96	11.16	1.31	0.00	1.02	0.00	22.59	99.31	71.2
6	1.43	0.90	5.61	42.96	22.76	11.55	11.21	1.06	0.00	0.70	0.00	22.45	97.87	69.3
7	1.28	0.90	5.90	42.94	23.58	11.99	11.60	1.00	0.00	0.81	0.00	22.02	98.43	68.4
8	0.64	0.74	6.05	47.44	17.90	8.83	9.07	1.33	0.00	0.93	0.00	24.78	99.81	72.9
9	0.81	0.63	5.83	46.51	18.59	8.47	10.12	1.00	0.00	0.75	0.00	25.79	99.91	71.7
10	1.02	0.97	6.46	43.63	21.09	11.05	10.03	1.09	0.00	0.71	0.00	22.68	97.65	69.5
11	0.75	0.91	6.81	45.31	17.81	8.62	9.19	1.46	0.00	0.88	0.00	24.93	98.86	70.6
12	0.53	0.76	5.90	47.23	16.74	8.01	8.73	1.08	0.00	0.78	0.00	25.55	98.57	73.4
13	0.89	0.81	5.70	46.31	19.73	9.81	9.92	1.43	0.00	1.67	0.00	22.91	99.45	72.1
14	0.55	0.50	5.31	47.79	15.17	6.65	8.52	1.12	0.00	1.10	0.00	27.25	98.79	74.9
15	0.73	0.63	5.78	48.53	17.46	9.27	8.19	0.91	0.00	0.64	0.00	25.00	99.68	74.7
16	0.95	0.82	5.23	47.05	18.28	8.97	9.31	0.86	0.00	0.73	0.00	25.39	99.31	73.8
17	0.91	0.81	5.76	44.69	18.80	10.01	8.79	1.13	0.00	1.24	0.00	22.14	95.48	72.5
18	0.81	0.66	5.88	44.23	17.55	8.24	9.32	0.88	0.00	0.65	0.00	24.76	95.42	71.5
19	1.07	0.87	6.12	44.47	20.09	9.87	10.22	1.52	0.00	0.96	0.00	23.47	98.57	70.2
20	0.55	0.68	6.65	45.97	16.14	7.18	8.96	1.41	0.00	1.00	0.00	25.83	98.23	71.4
21	0.71	0.63	5.49	45.98	17.70	8.08	9.63	1.31	0.00	1.17	0.00	24.41	97.40	72.6
22	0.83	0.86	6.02	46.26	18.40	8.90	9.50	1.31	0.00	0.92	0.00	24.87	99.47	72.0
23	1.39	0.79	5.29	44.82	21.97	11.93	10.04	0.98	0.00	0.69	0.00	22.02	97.95	72.0
24	0.53	0.26	8.15	46.85	13.39	5.86	7.53	1.20	0.00	0.95	0.00	27.86	99.19	70.8
25	1.23	1.03	5.98	45.52	21.16	11.98	9.18	1.03	0.00	1.08	0.00	22.02	99.05	72.1
26	0.43	0.62	6.16	49.09	12.77	5.35	7.42	1.01	0.00	1.06	0.00	28.45	99.59	75.1
Mean	0.90	0.76	5.92	45.67	18.83	9.29	9.54	1.16	0.00	0.91	0.00	24.27	98.43	71.8
Max	1.55	1.03	8.15	49.09	25.34	13.23	12.11	1.52	0.00	1.67	0.00	28.45	99.91	75.4
Min	0.43	0.26	5.12	41.96	12.77	5.35	7.42	0.86	0.00	0.49	0.00	20.70	94.03	67.6

Loftarstone AlC grains

#	TiO_2	V_2O_3	Al_2O_3	Cr_2O_3	FeO total	FeO	Fe_2O_3	MnO	MgO	Cu_2O	NiO	ZnO	Tot.	Cr#
1	0.51	0.00	16.55	42.03	36.35	31.17	5.18	1.29	1.13	0.00	0.24	0.00	98.10	58.7
2	0.16	0.00	13.89	50.68	26.09	22.44	3.65	2.08	6.03	0.00	0.18	0.00	99.11	67.7
Mean	0.34	0.00	15.22	46.36	31.22	26.80	4.42	1.69	3.58	0.00	0.21	0.00	98.60	63.2

Brecciated dolerite dyke grains

#	TiO_2	V_2O_3	Al_2O_3	Cr_2O_3	FeO total	FeO	Fe_2O_3	MnO	MgO	Cu_2O	NiO	ZnO	Tot.	Cr#
1	0.89	0.18	5.08	38.66	50.29	29.44	20.85	1.47	0.35	0.00	0.00	1.73	98.65	58.5
2	0.92	0.18	4.30	38.25	51.12	29.72	21.40	1.44	0.25	0.00	0.00	1.15	97.61	58.8
Mean	0.91	0.18	4.69	38.46	50.71	29.58	21.12	1.46	0.30	0.00	0.00	1.44	98.13	58.7

[1]Cr#: mole% Cr/(Cr+Al+Fe^{3+})